

Molecular-level Understanding of Optimizing Reaction Paths for Shape Concerning the Metal-support Interaction Effect of Co/CeO₂ on Water-Gas Shift Catalysis

Yingying Zhan, Yi Liu, Xuanbei Peng, Yongfan Zhang, Yanning Cao, Chak-tong Au
and Lilong Jiang*

National Engineering Research Center of Chemical Fertilizer Catalyst, Fuzhou University, Fuzhou, Fujian 350002, China. Corresponding author E-mail: jll@fzu.edu.cn/jllfzu@sina.cn

1. Results

Co/CeO₂-R (Figure 1B) show a diameter of 11.8±1nm (Figure 1C). HR-TEM image (Figure 1D) displays that Co/CeO₂-R mainly has exposed (111) and (110) planes with *d*-spacing of 0.313 and 0.191 nm, respectively. The observation is consistent with the FFT result (Figure 1E). Co/CeO₂-Sph is composed of uniform nanospheres 162 nm in size (Figure 1F–H). Notably, the spheres are made up of tiny close-packed nanoplates (Figure 1H), and the HR-TEM image of Figure 1I displays clear (111) and (110) lattice fringes with interplanar spacing of 0.313 and 0.191 nm, respectively. Co/CeO₂-C (Figure 1K–L) is composed of nanocubes 17–48 nm in size (Figure 1M). The inter planar spacings (*d*-spacing) of 0.256 and 0.192 nm confirm the presence of (100) and (110) planes on the surfaces. The Co/CeO₂-Spi sample shows spindles having length of 3–12 μm and width of 0.8–2.6 μm (Figure 1P). The sharp ends and curved edges of the spindles suggest the existence of defect sites (Figure 1S). The spindles have exposed (111) and (100) planes (Figure 1O). It is noted that the lattice fringes associated with Co₃O₄ are not observed for all Co/CeO₂ samples, indicating good dispersion of Co₃O₄ on CeO₂,¹ as proven by STEM-mapping and line scanning.

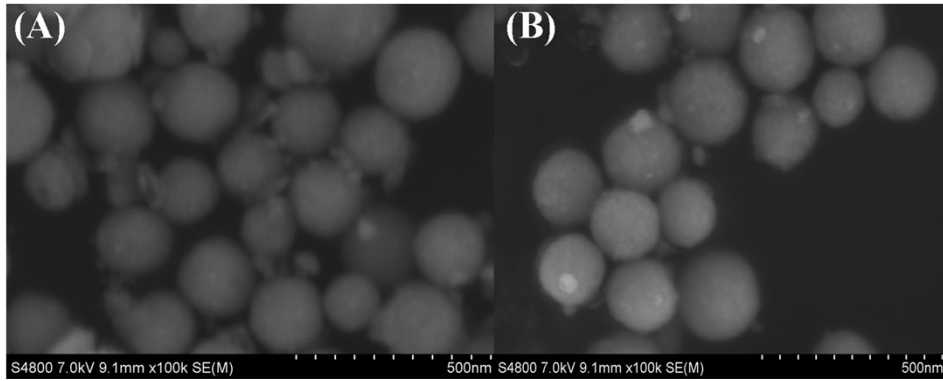


Figure S1 (A) SEM image of Co/CeO₂-Sph after WGS activity test. (B) SEM image of Co/CeO₂-Sph after WGS activity test and then maintained at 400 °C for 30 h.

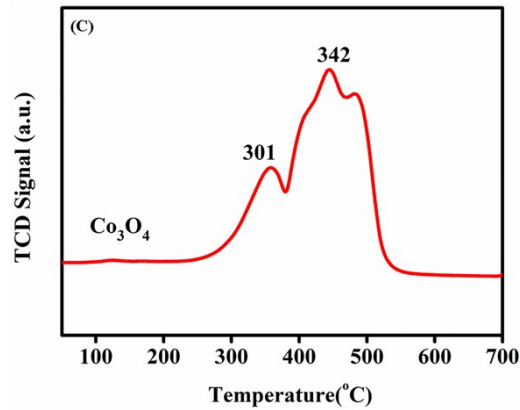


Figure S2 H₂-TPR profiles of (A) CeO₂ support; (B) Co/CeO₂ catalyst and (C) pure Co₃O₄.

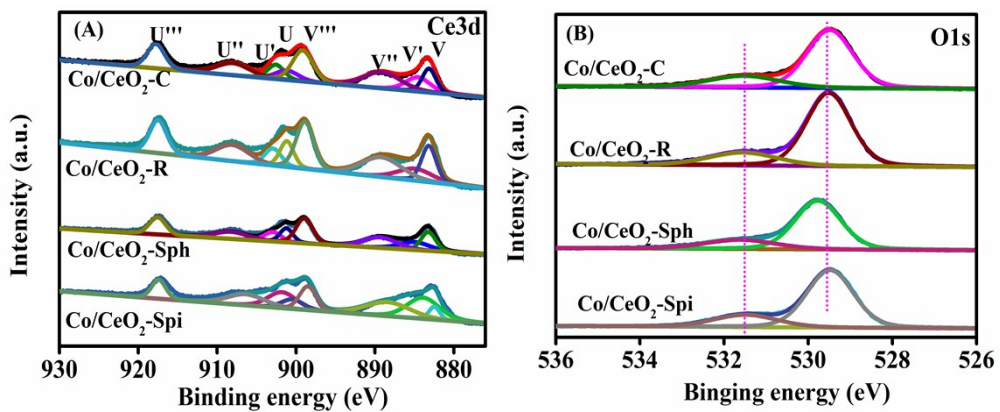


Figure S3 XPS spectra of fresh Co/CeO₂ catalysts (A) Ce3d and (B) O1s.

For Ce3d XPS spectra (Figure S5A), the peaks assigned U' and V' are indicative of the 3d¹⁰4f¹ initial electronic configuration matching well with surface Ce³⁺ species, while the peaks assigned U, U'', U''', V, V'' and V''' are the representative of the 3d¹⁰4f⁰ electronic configuration corresponding to surface Ce⁴⁺ species.^{1,2} The ratio of Ce³⁺/Ce is calculated and the results are given in Table S2. The surface Ce³⁺ concentrations in four Co-CeO₂ catalysts is about 25-27 % with only minor variations among the different morphologies. The existence of Ce³⁺ species could cause a charge imbalance and unsaturated chemical bonds on the catalyst surface, thereby giving rise to the promotion of surface oxygen vacancies. Concerning the type of oxygen species that could be involved in the redox or associative mechanisms,^{3,4} O1s XPS spectra of catalysts are shown in Figure S5B. The peak at 529.4-529.7 eV can be assigned to lattice oxygen (O_{latt}),^{5,6} while the one at 531.4-531.6 eV can be assigned to surface adsorbed oxygen species (O_{ads}), resulting from the adsorption of gaseous O₂ into oxygen vacancies.⁸ The O_{ads}/(O_{ads} + O_{latt}) ratio in untreated Co₃O₄-CeO₂ catalysts is about 21-23% (Table S2) also with only minor variations among the different morphologies.

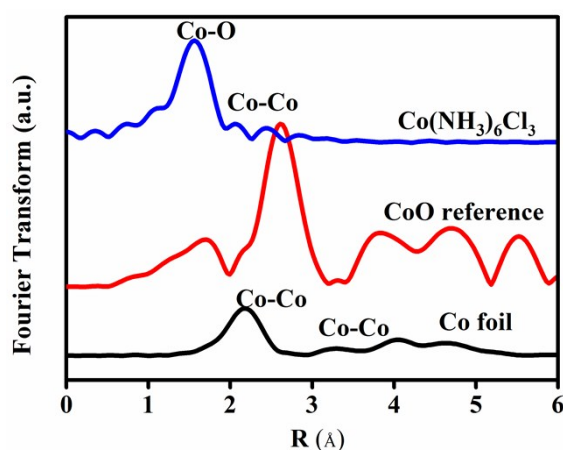


Figure S4 EXAFS spectra of Co-K edge over reference samples.

Table S1 Reaction temperature, Ce⁴⁺/Ce, Ce³⁺/Ce and O_{ads}/(O_{latt}+O_{ads}) ratio.

Catalysts	T _{90%} (°C)	Ce ⁴⁺ /Ce (%)	Ce ³⁺ /Ce (%)	O _{ads} /(O _{ads} +O _{latt}) (%)
Co/CeO ₂ -C	372	74.4	25.6	23
Co/CeO ₂ -R	383	72.7	27.3	21
Co/CeO ₂ -Sph	298	73.2	26.8	25
Co/CeO ₂ -Spi	-	74.4	25.6	22

Table S2 Surface Co concentration and O_{ads}/(O_{ads}+O_{latt}) ratio of Co/CeO₂-Sph catalysts at different WGS reaction temperatures.

Sample	Surface Co concentration (%)	O _{ads} /(O _{ads} +O _{latt}) (%)
Co/CeO ₂ -Sph-Fresh	7.50	25
Co/CeO ₂ -Sph (200 °C)	7.35	41
Co/CeO ₂ -Sph (300 °C)	7.18	50
Co/CeO ₂ -Sph (400 °C)	5.47	58

References

1. B. C. Rivas, J. I. Gutiérrez-Ortiz, Morphology-dependent properties of Co₃O₄/CeO₂ catalysts for low temperature dibromomethane (CH₂Br₂) oxidation. *J. Catal.* 281 (2011) 88–97.
2. D. Carta, A. Corrias, A Structural and magnetic investigation of the inversion degree in ferrite nanocrystals MFe₂O₄ (M = Mn, Co, Ni). *J. Phys. Chem. C* 113(2009) 8606–8615.
3. S. Zhang, F. (Feng). Tao, WGS catalysis and in situ studies of CoO_{1-x}, PtCo_n/Co₃O₄, and Pt_mCo_m/CoO_{1-x} nanorod catalysts. *J. Am. Chem. Soc.* 135(2013) 8283–8293.
4. D. Gamarra, A. Martínez-Arias, Selective CO oxidation in excess H₂ over copper-ceria catalysts: identification of active entities/species. *J. Am. Chem. Soc.* 129 (2007) 12064–12065.
5. Y. Liu, G. Guo, Mesoporous Co₃O₄-supported gold nanocatalysts: highly active for the oxidation of carbon monoxide, benzene, toluene, and o-xylene. *J. Catal.* 309(2014) 408–

418 (2014).

6. J. Xu, S.C. Tsang, Size dependent oxygen buffering capacity of ceria nanocrystals. *Chem. Commun.* 46(2010) 1887–1889.